Applied Physics Letters

RESEARCH ARTICLE | SEPTEMBER 10 2024

Gallium nitride-based resonant tunneling diode oscillators

FREE

Masahiro Murayama ; Hisayoshi Motobayashi; Yukio Hoshina; Miwako Shoji; Yoshiro Takiguchi ; Hiroyuki Miyahara; Takahiro Koyama ; Noriyuki Futagawa

Appl. Phys. Lett. 125, 113503 (2024)
https://doi.org/10.1063/5.0225312

AIP Publishing

Applied Physics Letters ARTICLE pubs.aip.org/aip/apl

Gallium nitride-based resonant tunneling diode oscillators

Cite as: Appl. Phys. Lett. **125**, 113503 (2024); doi: 10.1063/5.0225312
Submitted: 24 June 2024 · Accepted: 24 August 2024 ·
Published Online: 10 September 2024

Masahiro Murayama,[a] Hisayoshi Motobayashi, Yukio Hoshina, Miwako Shoji, Yoshiro Takiguchi, Hiroyuki Miyahara, Takahiro Koyama, and Noriyuki Futagawa

AFFILIATIONS

Compound Semiconductor Development Department, Sony Semiconductor Solutions Corporation, Atsugi-shi, Kanagawa 243-0014, Japan

[a]Author to whom correspondence should be addressed: Masahiro.Murayama@sony.com

ABSTRACT

We demonstrated GaN-based resonant tunneling diode (RTD) oscillators employing monolithic microwave integrated circuits. The GaN-based RTDs with a GaN quantum well and AlN double barriers were grown on freestanding c-plane semi-insulating GaN substrates using metal–organic chemical vapor deposition. The circuit components, including an RTD, a coplanar waveguide, a metal–insulator–metal capacitor, and shunt resistors, were monolithically fabricated on the GaN substrate. The circuits oscillated at a fundamental frequency of 17 GHz, which closely matched an estimated frequency using a three-dimensional electromagnetic simulator and a circuit simulator. This study contributes to the advancement of semiconductor high-frequency devices for millimeter wave and terahertz applications.

Resonant tunneling diodes (RTDs) enable high-frequency and high-power oscillators and stand out as strong candidates for millimeter wave and terahertz sources. RTD oscillators have been studied mainly using III-arsenide, phosphide, and antimonide materials. InGaAs/AlAs RTD oscillators reached approximately 2 THz in the fundamental frequency,[1] and their output powers have increased up to levels approximating milliwatts.[2–5] To further increase the output, studies have also been conducted on RTD oscillator arrays, and recently, the highest record output of 11.8 mW was reported in a 36-element oscillator array.[6]

III-nitride materials, which have attractive properties, such as wideband offset, high thermal conductivity, high breakdown voltage, and other properties, have the potential to realize high-power and highly reliable RTD oscillators. Several groups have studied GaN-based RTDs for several decades. The first GaN-based RTD was reported in 2001;[7] however, early stage research faced challenges as it lacked reproducibility in the current–voltage (I–V) characteristics, where the negative differential resistance (NDR) disappeared during the repeated I–V measurements.[8–14] Recently, GaN-based RTDs with stable NDR actions have been reported,[15–20] and they have approached practical levels in terms of peak current densities and peak-to-valley current ratios (PVCRs).[21–23] Several studies have been conducted to realize GaN-based RTD oscillators, including evaluations of the RTD response performance,[24] and demonstrations of oscillation using the RTD connected to external circuits.[25] However, monolithically fabricated GaN-based RTD oscillators are yet to be achieved.

RTDs require precise thickness control and crystal quality of quantum wells and barriers for effective resonant tunneling. Therefore, most RTD research, including nitride and arsenide materials, has been conducted using the molecular beam epitaxy (MBE) method, allowing for greater precise thickness control than metal–organic chemical vapor deposition (MOCVD). Although, as required to attain favorable RTD characteristics, achieving accurate control of layer thickness at the atomic level and abrupt heterointerface between the well and barrier layers is challenging, MOCVD is known for its high productivity and ability to produce high-quality crystals, making it suitable for various compound semiconductor devices, including optical and electronic devices. If the growth conditions are established in MOCVD, favorable RTD characteristics can be expected.

However, monolithic microwave integrated circuit (MMIC)-based RTD oscillators have been previously studied with InGaAs/AlAs RTDs.[26–28] By employing them for GaN RTDs, it is possible to electrically evaluate the oscillation characteristics, enabling the assessment of a wide range of oscillation frequencies without special evaluation methods.

In this Letter, we demonstrate a GaN-based RTD grown using the MOCVD method and its oscillators employing MMICs.

The GaN-based RTD epitaxial structure incorporated a GaN quantum well and AlN double barriers with a thickness of 2.0 and

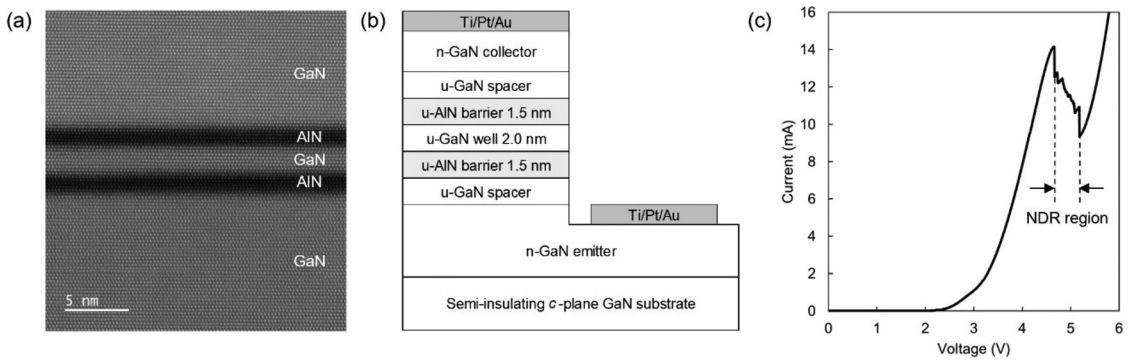

FIG. 1. (a) STEM image of AlN/GaN/AlN well and barriers grown using MOCVD, (b) schematic of fabricated GaN/AlN RTD structure, and (c) representative I–V characteristics for GaN/AlN RTD with a 3 μm diameter mesa.

1.5 nm, respectively. This structure was grown on freestanding c-plane semi-insulating GaN substrates using the MOCVD method. To enhance controllability and crystallinity even in MOCVD, we optimized the growth conditions and employed heterointerface treatment techniques. These efforts achieved preferable AlN/GaN/AlN ultra-thin films, as shown in the scanning transmission electron microscopy (STEM) image in Fig. 1(a). The RTD structure, as illustrated in Fig. 1(b), was fabricated with a mesa structure formed by a dry etching method. Ti/Pt/Au was deposited as a collector and emitter electrode on top of the mesa and the bottom, respectively. Figure 1(c) shows the representative I–V characteristics for the GaN/AlN RTD sample with a 3 μm diameter mesa. An NDR region was observed in the voltage range from 4.7 to 5.2 V, which had a peak current density of approximately 200 kA/cm^2 and a PVCR of 1.52. In the RTD oscillator circuit, the negative resistance of the RTD serves as gain, counteracting the power consumption of the circuit and sustaining oscillation. Therefore, the negative conductance of the RTD should be greater than that of the circuit. The negative differential conductance, expressed as (3/2) ($\Delta I/\Delta V$), was calculated to be 14 mS, where ΔI and ΔV are defined as the difference between the peak and valley current and peak and valley voltage, respectively, in the NDR region.[29] The RTD exhibited excellent repeatability of I–V characteristics and was expected to operate stably as negative resistance elements in oscillators.

Figure 2(a) is a schematic of the fabricated GaN RTD-based MMIC oscillator. The device included an RTD with a 3 μm diameter mesa, metal–insulator–metal (MIM) capacitor, coplanar waveguide (CPW), and shunt resistors. These circuit components were monolithically fabricated on the semi-insulating GaN substrates using standard device processing methods. The MIM capacitor employed a 200 nm thick SiO_2 layer sandwiched by a signal and ground metal consisting of Ti/Pt/Au. The signal and ground metal doubled as the collector and emitter electrodes of the RTD. The shunt resistors, which contributed to suppressing parasitic oscillations in the circuit and stabilizing the intended oscillation, were formed by selectively leaving the n-GaN emitter layer without etching. The equivalent circuit of the device is shown in Fig. 2(b). The RTD is represented as a parallel circuit of a negative conductance $-G_d$ and capacitance C_d. L_w is the inductance of the CPW, C_c is the capacitance of the MIM capacitor, and G_s is the conductance of the shunt resistors. The resistance of the transmission line, capacitance of the CPW, and various other circuit components are omitted here for simplification. Because the MIM capacitor was designed to cut off DC or low-frequency signals and pass high-frequency signals, it can be considered as a short circuit for the intended RF signal such that the equivalent circuit shown in Fig. 2(b)

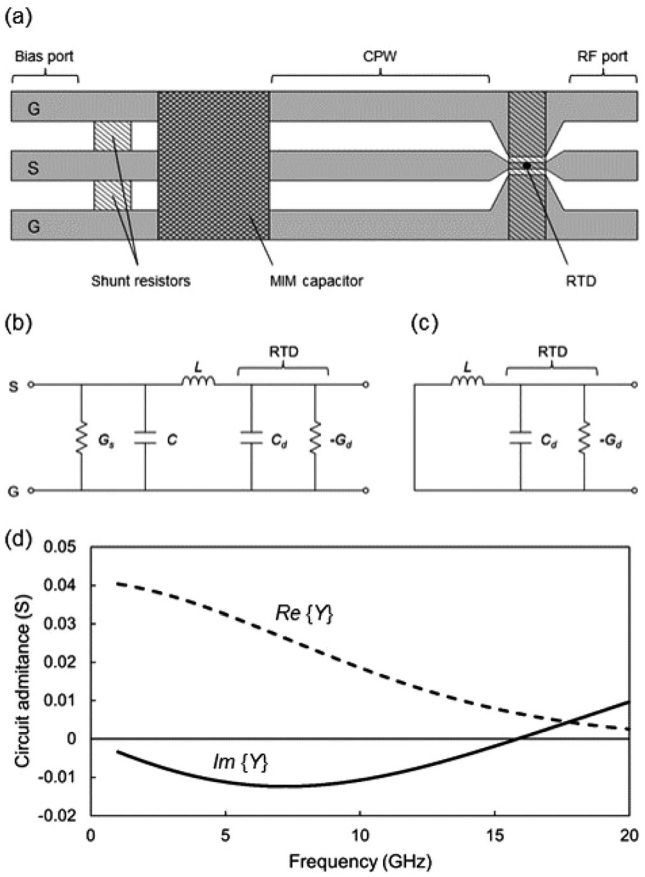

FIG. 2. (a) Schematic of GaN RTD-based MMIC oscillator, (b) equivalent circuit of device, (c) simplified equivalent circuit for RF signal, and (d) frequency dependence of circuit admittance, including RTD calculated using HFSS and ADS.

can be simplified as shown in Fig. 2(c). Thus, the oscillation frequency is largely determined by L_w and C_d. The area of the MIM and the length of the CPW, which determine the cutoff frequency and inductance of the circuit, respectively, were calculated using a three-dimensional (3D) electromagnetic simulator (Ansys HFSS) and circuit simulator (Keysight ADS) to achieve an oscillation frequency in the range of 10–20 GHz. Figure 2(d) shows the frequency dependence of the circuit admittance, including the RTD circuit information. The oscillation frequency was estimated to be approximately 16 GHz, where the imaginary part of the admittance $Im\{Y\}$, that is, the susceptance of the circuit becomes zero. At the estimated oscillation frequency, as the conductance of the circuit, $Re\{Y\}$, of 6.6 mS is sufficiently smaller compared to the negative differential conductance of the RTD of 14 mS, the RTD is expected to work as a negative resistance component to cancel the parasitic resistance of the oscillation circuit.

The oscillation frequency of the fabricated circuit was measured on-wafer using a spectrum analyzer. GSG probes were used to apply DC voltage to the device from one side [the left side of the device in Fig. 2(a)] and prove the oscillation from the other (the right side). The measured spectrum is shown in Fig. 3. The oscillation was successfully achieved at a fundamental frequency of approximately 17 GHz, which mostly corresponds to the frequency estimated in the simulation. The inset of the figure displays the I–V characteristics of the device. The I–V curve is represented by the sum of the current components flowing through the RTD and shunt resistors. The applied voltage to measure the oscillation spectrum was set at the center of the NDR region. At higher frequencies, the RTD characteristics, such as the negative differential conductance, contact resistance, and sheet resistance, must be improved, and the oscillator design must be optimized. These improvements of the RTD characteristics are expected to be achieved by optimizing the crystal structures, MOCVD growth conditions, and process conditions.

In conclusion, we developed GaN-based RTD oscillators to realize high-power and highly reliable sources for millimeter wave and terahertz applications, and we have demonstrated the GaN-based RTD and its oscillator with a fundamental frequency of 17 GHz. The GaN/AlN RTD was grown using MOCVD with precise thickness control and abrupt well/barrier heterointerfaces. The oscillation circuits included the RTD with a 3 μm diameter mesa, CPW, MIM capacitor, and shunt resistors monolithically integrated on the semi-insulating GaN substrate. The oscillation circuit was designed using a 3D electromagnetic simulator HFSS and circuit simulator ADS, and the estimated oscillation frequency closely matched the experimental results. To further improve the oscillation characteristics, a dual approach that focuses on both improving the RTD characteristics and optimizing the oscillator design is required. It is expected that further improvements of the RTD characteristics can be achieved by optimizing the crystal structures, MOCVD growth conditions, and process conditions. III-nitride semiconductors are highly attractive materials, paving the way for future high-output and highly reliable RTD oscillators. Advancements in GaN-based RTD oscillators will certainly contribute to the further popularizing of millimeter wave and terahertz sources.

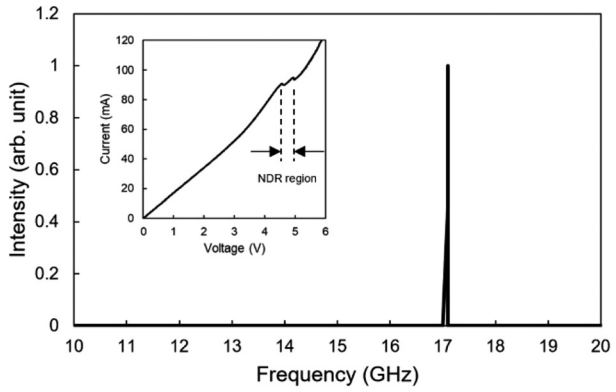

FIG. 3. Oscillation spectrum of GaN RTD-based MMIC oscillator when applying DC bias around the center of NDR region. Inset shows I–V characteristics of RTD with shunt resistors.

AUTHOR DECLARATIONS

Conflict of Interest

The authors have no conflicts to disclose.

Author Contributions

Masahiro Murayama: Conceptualization (lead); Data curation (lead); Formal analysis (lead); Investigation (equal); Methodology (lead); Project administration (lead); Validation (lead); Visualization (lead); Writing – original draft (lead); Writing – review & editing (lead). **Hisayoshi Motobayashi:** Conceptualization (equal); Data curation (equal); Formal analysis (equal); Investigation (equal); Software (lead); Validation (equal); Visualization (equal). **Yukio Hoshina:** Conceptualization (equal); Methodology (equal); Validation (equal). **Miwako Shoji:** Methodology (equal); Validation (equal). **Yoshiro Takiguchi:** Formal analysis (equal); Validation (equal). **Hiroyuki Miyahara:** Data curation (equal); Validation (equal). **Takahiro Koyama:** Funding acquisition (equal); Supervision (equal); Writing – review & editing (equal). **Noriyuki Futagawa:** Funding acquisition (equal); Supervision (equal); Writing – review & editing (equal).

DATA AVAILABILITY

The data that support the findings of this study are available from the corresponding author upon reasonable request.

REFERENCES

[1]R. Izumi, S. Suzuki, and M. Asada, in *42nd International Conference on Infrared, Millimeter, and Terahertz Waves (IRMMW-THz)* (IEEE, 2017).
[2]F. Han, T. Shimura, H. Tanaka, and S. Suzuki, Appl. Phys. Express **16**, 064003 (2023).
[3]T. V. Mai, M. Asada, T. Namba, Y. Suzuki, and S. Suzuki, IEEE Trans. Terahertz Sci. Technol. **13**, 405 (2023).
[4]H. Tanaka, H. Fujikata, F. Han, and S. Suzuki, Jpn. J. Appl. Phys., Part 1 **63**, 011004 (2024).
[5]S. Endo and S. Suzuki, Appl. Phys. Express **17**, 044001 (2024).
[6]Y. Koyama, Y. Kitazawa, K. Yukimasa, T. Uchida, T. Yoshioka, K. Fujimoto, T. Sato, J. Iba, K. Sakurai, and T. Ichikawa, IEEE Trans. Terahertz Sci. Technol. **12**, 510 (2022).
[7]A. Kikuchi, R. Bannai, and K. Kishino, Phys. Status Solidi A **188**(1), 187 (2001).
[8]C. T. Foxon, S. V. Novikov, A. E. Belyaev, L. X. Zhao, O. Makarovsky, D. J. Walker, L. Eaves, R. I. Dykeman, S. V. Danylyuk, S. A. Vitusevich, M. J. Kappers, J. S. Barnard, and C. J. Humphreys, Phys. Status Solidi C **0**(7), 2389 (2003).

[9]S. Golka, C. Pflügl, W. Schrenk, G. Strasser, C. Skierbiszewski, M. Siekacz, I. Grzegory, and S. Porowski, Appl. Phys. Lett. **88**, 172106 (2006).
[10]S. Leconte, S. Golka, G. Pozzovivo, G. Strasser, T. Remmele, M. Albrecht, and E. Monroy, Phys. Status Solidi C **5**(2), 431–434 (2008).
[11]C. Bayram, Z. Vashaei, and M. Razeghi, Appl. Phys. Lett. **96**, 042103 (2010).
[12]C. Bayram, Z. Vashaei, and M. Razeghi, Appl. Phys. Lett. **97**, 181109 (2010).
[13]S. Sakr, E. Warde, M. Tchernycheva, L. Rigutti, N. Isac, and F. H. Julien, Appl. Phys. Lett. **99**, 142103 (2011).
[14]M. Boucherit, A. Soltani, E. Monroy, M. Rousseau, D. Deresmes, M. Berthe, C. Durand, and J.-C. De Jaeger, Appl. Phys. Lett. **99**, 182109 (2011).
[15]T. A. Growden, D. F. Storm, W. Zhang, E. R. Brown, D. J. Meyer, P. Fakhimi, and P. R. Berger, Appl. Phys. Lett. **109**, 083504 (2016).
[16]D. F. Storm, T. A. Growden, W. Zhang, E. R. Brown, N. Nepal, D. S. Katzer, M. T. Hardy, P. R. Berger, and D. J. Meyer, J. Vac. Sci. Technol. B **35**, 02B110 (2017).
[17]T. A. Growden, W. Zhang, E. R. Brown, D. F. Storm, K. Hansen, P. Fakhimi, D. J. Meyer, and P. R. Berger, Appl. Phys. Lett. **112**, 033508 (2018).
[18]J. Encomendero, F. A. Faria, S. M. Islam, V. Protasenko, S. Rouvimov, B. Sensale-Rodriguez, P. Fay, D. Jena, and H. G. Xing, Phys. Rev. X **7**, 041017 (2017).
[19]D. Wang, Z. Y. Chen, T. Wang, L. Y. Yang, B. W. Sheng, H. P. Liu, J. Su, P. Wang, X. Rong, J. Y. Cheng, X. Y. Shi, W. Tan, S. P. Guo, J. Zhang, W. K. Ge, B. Shen, and X. Q. Wang, Appl. Phys. Lett. **114**, 073503 (2019).
[20]D. Wang, J. Su, Z. Chen, T. Wang, L. Yang, B. Sheng, S. Lin, X. Rong, P. Wang, X. Shi, W. Tan, J. Zhang, W. Ge, B. Shen, Y. Liu, and X. Wang, Adv. Electron. Mater. **5**, 1800651 (2019).
[21]T. A. Growden, D. F. Storm, E. M. Cornuelle, E. R. Brown, W. Zhang, B. P. Downey, J. A. Roussos, N. Cronk, L. B. Ruppalt, J. G. Champlain, P. R. Berger, and D. J. Meyer, Appl. Phys. Lett. **116**, 113501 (2020).
[22]H. Zhang, J. Xue, Y. Fu, L. Li, Z. Sun, J. Yao, F. Liu, K. Zhang, X. Ma, J. Zhang, and Y. Hao, J. Appl. Phys. **129**, 014502 (2021).
[23]H. Zhang, J. Xue, Z. Sun, L. Li, J. Yao, F. Liu, X. Yang, G. Wu, Z. Li, Y. Fu, Z. Liu, J. Zhang, and Y. Hao, Appl. Phys. Lett. **119**, 153506 (2021).
[24]W.-D. Zhang, T. A. Growden, D. F. Storm, D. J. Meyer, P. R. Berger, and E. R. Brown, IEEE Trans. Electron Devices **67**(1), 75 (2020).
[25]J. Encomendero, R. Yan, A. Verma, S. M. Islam, V. Protasenko, S. Rouvimov, P. Fay, D. Jena, and H. G. Xing, Appl. Phys. Lett. **112**, 103101 (2018).
[26]J. Wang, K. Alharbi, A. Ofiare, H. Zhou, A. Khalid, D. Cumming, and E. Wasige, in IEEE Compound Semiconductor Integrated Circuit Symposium (CSICS), 2015.
[27]A. C. Cornescu, R. Morariu, A. Ofiare, A. Al-Khalidi, J. Wang, J. M. L. Figueiredo, and E. Wasige, IEEE Trans. Microwave Theory Tech. **67**(8), 3449 (2019).
[28]A. Al-Khalidi, K. H. Alharbi, J. Wang, R. Morariu, L. Wang, A. Khalid, J. M. L. Figueiredo, and E. Wasige, IEEE Trans. Terahertz Sci. Technol. **10**(2), 150 (2020).
[29]N. Orihashi, S. Hattori, S. Suzuki, and M. Asada, Jpn. J. Appl. Phys., Part 1 **44**(11), 7809 (2005).